Control Theory Prediction of Resolved Cheyne-Stokes Respiration in Heart Failure

Supplemental Data

Scott A. Sands[1,2,3,4*], Bradley A. Edwards[3,5,6], Kirk Kee[1,2], Christopher Stuart-Andrews[1], Elizabeth M. Skuza[4], Teanau Roebuck[1], Anthony Turton[7], Garun S. Hamilton[7,8], Matthew T. Naughton[1,2], Philip J. Berger[4]

[1]General Respiratory and Sleep Medicine, Department of Allergy, Immunology and Respiratory Medicine, The Alfred, Melbourne, Australia.
[2]Central Clinical School, Monash University, Melbourne, Australia.
[3]Sleep Disordered Breathing Laboratory, Division of Sleep and Circadian Disorders, Departments of Medicine and Neurology, Brigham and Women's Hospital and Harvard Medical School, Boston, USA.
[4]The Ritchie Centre, Hudson Institute of Medical Research, Monash University, Melbourne, Australia.
[5]Sleep and Circadian Medicine Laboratory, Department of Physiology, Monash University, Melbourne, Australia.
[6]School of Psychological Sciences and Monash Institute of Cognitive and Clinical Neurosciences, Monash University, Melbourne, Australia.
[7]Monash Lung and Sleep, Monash Medical Centre, Melbourne, Australia.
[8]School of Clinical Sciences, Monash University, Melbourne, Australia.

THEORY

Control theory background

The essential features of the control theory framework describing ventilatory instability and Cheyne-Stokes respiration have been described in detail elsewhere [S1-4] and are summarised for convenience in Figure S1. It is helpful to consider a transient (sinusoidal) disturbance to ventilation, shown in the form of a hypopnea (Figure S1a). This reduction in ventilation acts on the *plant* to decrease the rate of CO_2 excretion from the lungs and therefore provides a transient increase in $PACO_2$ (and to the arterial PCO_2). Likewise there will be a reduction in alveolar and arterial PO_2. After the affected arterial blood has been transported from the lungs to the peripheral and central chemoreceptors (i.e. after the circulation delay), the rise in PCO_2 is sensed by the chemoreceptors (the controller) whose combined effect generates an increase in ventilatory drive in response to the increase in PCO_2.

Definition of ventilatory drive. Ventilatory drive is defined here as the chemical stimulus to breathe (e.g. local chemoreceptor PCO_2/H^+) in units of ventilation. Ventilatory drive is equal to ventilation except when PCO_2 falls below the apnoeic threshold; at this time, while ventilation is zero, ventilatory drive tracks PCO_2 as it swings below the apnoeic threshold, and therefore reflects the additional chemical stimulus needed to restore breathing. Unlike ventilation, ventilatory drive (as defined here) maintains a proportional relationship to PCO_2 throughout the CSR cycle.

What is loop gain? The ratio of the magnitude of the ventilatory drive response to the size of the ventilatory disturbance is known as *loop gain*. If loop gain is <1 the system is stable, but if loop gain is >1, then each response will be larger than the prior disturbance, yielding progressive oscillatory growth (Figure S1b) and ultimately cyclic CSA.

Factors influencing loop gain

The following equation encapsulates the factors influencing loop gain [S3, S4], and forms the basis for predicting the size of the intervention required to reduce loop gain below a value of 1 and achieve stable breathing:

$$\text{Loop gain} = G\left[\frac{PACO_2 - PICO_2}{\text{lung volume}}T\right] \qquad \text{Equation S1}$$

where G = chemosensitivity (*controller gain*; ratio of ΔV_{drive} to swings in alveolar PCO_2 [$\Delta PACO_2$]), and the remaining terms comprise the *plant gain* defined as the ratio of swings in $PACO_2$ for any given fluctuation in V_E ($\Delta PACO_2/\Delta V_E$): $PACO_2 - PICO_2$ is the mean alveolar–inspired PCO_2 gradient, lung volume refers to the mean lung gas volume buffering $PACO_2$, and T is a complex timing factor encompassing circulatory delay. (Of note, T can be written as $T=[(2\pi/[\text{CSR cycle length}])^2+1/\tau_{plant}^2]^{-0.5}$ where τ_{plant} is the time constant of the plant [S3].)

In theory, once loop gain is known, Equation S1 can be used to determine the change in each of the terms necessary to reduce loop gain below 1. For example, if baseline loop gain is 1.8, then reducing $PACO_2 - PICO_2$ by 50% would lower loop gain on therapy ($LG_{therapy}$) to below 1.0 and should stabilise CSR. Doubling lung volume or halving chemosensitivity would have the same effect. The predictive utility of this theory is tested experimentally in the current study.

METHODS

Research polysomnography

Expired ventilation was measured via a sealed mask using two calibrated flow sensors placed in parallel to minimise airflow resistance (NICO, Novametrix, CT, USA). The total inspiratory and expiratory resistances of the circuit were 1.3 $cmH_2O/L.s$ and 2.3 $cmH_2O/L.s$ respectively at a flow rate of 30 L/min; at 60 L/min, resistances were 1.5 $cmH_2O/L.s$ and 2.8 $cmH_2O/L.s$. The CO_2 and O_2 in the inspired and expired air were assessed at the mask using rapid response gas analyzers (NICO, Novametrix, CT, USA; Ametek S-3A, AEI Technologies, TX, USA). Before gas mixtures were switched into the patient circuit, they were stored

temporarily at atmospheric pressure in 50 L Douglas bags and the CO_2 and O_2 concentrations entering the bags were set using separate gas analyzers (CO_2SMO Plus; Novametrix, CT, USA; AX300, Teledyne Analytical Instruments, CA, USA). Administration of inspired CO_2 was achieved by turning a three-way tap that switched the patient's inspiratory line from room air to the Douglas bag. Oesophageal manometry was also performed in 7 of 12 patients using a catheter (Millar, Houston TX, USA) inserted through a lidocaine-anesthetised nostril to sit in the lower two-thirds of the oesophagus to confirm central versus obstructive events.

Obtaining quality end-tidal PCO_2 data

Considerable effort was made to ensure only the highest quality end-tidal PCO_2 data were collected, such that it best reflects alveolar gas:

1.) Patients wore a sealed full-face mask to minimise the possibility of mouth leak.

2.) Mask gases (inspired and expired PCO_2/PO_2 waveforms) were sampled from the stream of oronasal inspired/expired gas by placing a sampling catheter through a dedicated mask sampling port such that the end of the catheter lay at an optimal position directly in front of both the nose and mouth.

3.) Gas was drawn through a sampling catheter at a flow rate of 1 L/min (using medical vacuum and a rotameter). This flow rate was chosen during preliminary testing by raising the flow rate to find the value after which there was no further improvement in the morphology of the CO_2 (and O_2) waveforms (considering the clarity of phase three alveolar plateaus and the sharpness of the inspiratory upstrokes and expiratory downstrokes). Of note this flow rate provided a negligible negative pressure in the mask (<0.025 cmH_2O) given the low resistance of the circuit (see above).

4.) The infrared CO_2 sensor was placed within 30 cm of the mask (<0.3 ml) to maximise the quality of the CO_2 waveform. The time between the mask PCO_2 and the sensor PCO_2 was <0.02 s. A greater volume of gas between the mask and the sensor can result in a reduced response time.

5.) End of expiration was detected using the ventilatory flow signal (via in-house software, MATLAB, Mathworks, Natick USA) that enabled manual correction of the precise time at which the end-tidal PCO_2 data were taken.

6.) Each individual end-tidal PCO_2 data point was manually inspected for validity before inclusion as an estimate of $PACO_2$. Values for breaths lower than deadspace (150 ml) were automatically excluded. Only breaths with clear alveolar plateaus were included; we report that no patient exhibited marked phase three alveolar slopes that would yield issues using end-tidal PCO_2 to reflect alveolar PCO_2.

Definition of established Cheyne-Stokes respiration

Inspired CO_2 was administered during periods of *established CSR* to:

1.) ensure that the baseline loop gain estimate is valid. In principle, the duty ratio method relies on a consistent CSR pattern with negligible growth or attenuation across cycles [S5, S6], and

2.) minimise the possibility that CSR would have spontaneously worsened or resolved, independent of the changes in CO_2.

Thus we defined established CSR as a 5 min epoch of CSR with:

1.) an oscillatory amplitude in ventilation that was not overtly rising or falling, reflected also in the absence of trends for changes in hyperpnoea duration and apnoea duration.

2.) the cycle duration was consistent, based on negligible differences in cycle duration within the epoch (below approximately 20% of the mean cycle duration).

Expected reduction in loop gain with inspired PCO_2

During quiet wakefulness, 3% inspired CO_2 was applied for 2 min (in duplicate) during stable breathing; $PACO_2 - PICO_2$ was taken as the average of breaths assessed in the last minute of the test and compared with the preceding 2 min baseline.

The change in $PACO_2$−$PICO_2$ per change in inspired CO_2 measured during wakefulness (*m*=18) and during CSR (*m*=18) was also the same as the value expected a priori from control theory and from the data of Lorenzi-Filho et al [S7]: from a baseline $PACO_2$ (awake arterial value) of 34.3 mmHg, $PACO_2$ (transcutaneous value) rose just 0.86 mmHg per 1% inspired CO_2 (1.6 mmHg with $FICO_2$ = 1.85%) to yield a value of *m*=18.

Inspired CO_2 administration during Cheyne-Stokes respiration

We note that the goal of administering inspired CO_2 during CSR was not to test whether inspired CO_2 resolves CSR as this a point already firmly established [S7-12]. Rather, the objective was to test whether control theory predicts CSR resolution.

Interventions that clearly resolved CSR were terminated after 5 min.

Baseline loop gain during Cheyne-Stokes respiration

Loop gain during baseline CSR ($LG_{baseline}$) was measured using the *duty ratio* (DR = ventilatory duration / cycle duration) which is uniquely related to the ratio of the size of sinusoidal swings in ventilatory drive (ΔV_{drive}) in response to those in ventilation (ΔV_E) [S5], as given by:

$$LG_{baseline} = \frac{\Delta V_{drive}}{\Delta V_E} = \frac{2\pi}{2\pi DR - \sin 2\pi DR} \qquad \text{Equation S2}$$

This equation is derived from decomposition of the feedback loop during CSR into non-linear and linear components [S5, S6]; it is the underlying linear component described here ($LG_{baseline}$) that determines the genesis and perpetuation of ventilatory oscillations [S5, S6] and which is influenced by $PACO_2$−$PICO_2$ and the other key factors described above (Eq. S1).

The duty ratio is illustrated in Figure S1 and Figure 2. Equation S2 is shown graphically in Figure S1b (inset). $LG_{baseline}$ was calculated using the median duty ratio in the 5 min preceding each intervention.

Confirming plant gain as the stabilizing mechanism of inspired CO_2

In order to confirm the stabilising mechanism of inspired CO_2, plant gain was measured by fitting a simplified 2-parameter lung model [S3] to end-tidal PCO_2 data that converts changes in ventilation ($\Delta V_E = V_E$ – mean V_E, V_E = tidal volume × breathing frequency; resampled at 4 Hz) into a continuous $PACO_2$ signal:

$$\tau \frac{dPACO_2}{dt} = -(PACO_2 - P_{eupnea}) - k(\Delta V_E) \qquad \text{Equation S3}$$

where k = gain, τ = lung time constant, P_{eupnea} = steady-state eupnoeic $PACO_2$; see Figure 2a. The median correlation coefficient of the fit was 0.94 at baseline and 0.87 during intervention. Plant gain was reported as the $PACO_2$ response to a 1 cycle/min fluctuation in V_E (plant gain = $k/[1+2\pi f\tau]^{0.5}$ where f=1 cycle/min).

To quantify the mean $PACO_2$−$PICO_2$ throughout the CSR cycle we used the model $PACO_2$ trace. Thus the average value of $PACO_2$ is estimated throughout the CSR cycle (apnoea and hyperpnoea), whereas only values during the ventilatory phase of the CSR cycle would be available if the end-tidal $PACO_2$ values were used; such a limitation would falsely lower the measured $PACO_2$−$PICO_2$.

Likewise, controller gain was measured by fitting a simplified relationship [S3] to V_E data that converts changes in $PACO_2$ ($\Delta PACO_2$) into changes in V_{drive}, given by:

$$\tau \frac{dV_{drive}}{dt} = -(V_{drive} - V_{eupnea}) + k \cdot \Delta PACO_2(t - \delta) \qquad \text{Equation S4}$$

where k is the slope of the ventilatory chemoreflex response to PCO_2, τ = controller time constant, δ = circulatory delay, V_{eupnea} = steady-state V_{drive} (when $\Delta PACO_2$=0). The V_{drive} signal (Equation S4) was fit to measured ventilation data (V_E) data when ventilation>0 (that is, ventilatory drive matches ventilation except during apnea). Note that circulatory delay is one of the model parameters (δ). The single time constant parameter captures the lumped effects of the major distortion effects of CO_2 mixing in the heart, vasculature, tissues, and neural distortion effects (time course of chemoreceptor response to local PCO_2) [S3]. Continuous $PACO_2$ data from Equation S3 (see Figure 2) were used as the input to Equation S4. Controller gain was reported as the ventilatory drive response to a 1 cycle/min fluctuation in $PACO_2$ (controller gain = $k/[1+2\pi f\tau]^{0.5}$ as above).

Note that plant gain and controller gain measurements are dependent on the frequency of the sinusoidal disturbance under investigation. Thus, measurements were made at a common frequency to enable plant gain and controller gain to be expressed in a way that is independent of the circulatory delay. Calculating plant gain and controller gain at the cycle period of CSR (using baseline cycle length for each intervention) did not alter the findings.

Our model-based approach to estimating plant and controller gain is based on previous studies using spontaneous ventilatory fluctuations [S13-15] and those induced by administration of dynamic inspired CO_2 stimulation [S16, S17] to characterise the ventilatory control system. We note that alternative methods to estimate controller gain (e.g. rebreathing hypercapnic ventilatory response, pseudorandom binary stimulation) would not be feasible during CSR in sleep, would interrupt the behaviour under investigation, and would not be as pertinent to CSR oscillations observed *in situ*.

Impact of sleep depth

On the basis that CO_2 is reported to promote arousal from sleep [S18], we sought to determine if arousals and sleep depth had a role in the resolution of CSR. We examined sleep efficiency (proportion of time without EEG arousals or wakefulness) and alpha EEG power (8-12 Hz, C3-A2 leads, 1 s windows, presented as % total power 1-16 Hz) during established CSR (5 min before each intervention) and during each intervention. Mean data were reported for each epoch at baseline and during CO_2 interventions.

RESULTS

Predicting persistent versus resolved Cheyne-Stokes respiration

Individual epochs. Since the analysis presented (Figure 3) contains repeated measurements from multiple patients, we also analysed the data using multiple logistic regression incorporating individual patients as categorical predictor variables to avert individual patient related bias. When individual patients were added to a regression model with baseline loop gain and inspired CO_2 level, baseline loop gain remained a significant

predictor of the response to intervention (before: P<0.001; after: P=0.003, see Tables S1-2); individual subjects did not significantly contribute to the predictive model. Likewise, a separate logistic regression examining $LG_{therapy}$ showed it remained a significant determinant of responses to intervention when individual patients were included (before: P<0.001; after: P<0.001).

Individualised m values. We tested whether accuracy of prediction was improved when we used individualised m values (range: 15-22) rather than the group average (m=18). Among the 8 subjects in whom m was measured during wakefulness, accuracy improved slightly to 85±5% (N=47/55; cutoff $LG_{therapy}$=0.9) using individual m values, compared to the accuracy of 80±4% using the group m value (N=76/95). Likewise, use of individualised m values taken from the CSR interventions also slightly improved the accuracy (84±4%, N=80/95).

Individual patients. Examining the pooled mean baseline loop gain categorised by persistent versus resolved CSR for each CO_2 level in each patient confirmed that there was a significantly greater baseline loop gain prior to persistent versus resolved CSR for 1% CO_2 (1.38±0.08 versus 1.11±0.04, p=0.03, N=5 and N=9 respectively) and 2% CO_2 (1.50±0.11 versus 1.23±0.06, p=0.03, N=9 and N=5 respectively).

The $FICO_2$ level required to resolve CSR on >50% of occasions in each patient was also recorded. Use of a single baseline loop gain value for each patient (median) revealed a strong but non-significant trend towards a higher baseline loop gain in the four individuals requiring 3% CO_2 to resolve CSR (N=4) versus those requiring ≤2% CO_2 (N=7): 1.41±0.11 versus 1.19±0.04 (mean±S.E.M.; p=0.067). Receiver operating characteristic analysis revealed excellent prediction (area under curve=0.82±0.14); the optimal baseline loop gain threshold of 1.30 accurately predicted the dose needed in 9/11 patients (good agreement; kappa = 0.61±0.25, where 0 represents chance agreement). Analysis using a single baseline loop gain value for each patient could only be performed in 11/12 patients; one patient's threshold CO_2 level was not determined due to insufficient CSR interventions.

Variability of baseline loop gain. Across epochs within individuals, the baseline loop gain values had a S.D. equal to 0.13±0.08 (mean±S.D.) and S.E.M. of 0.05±0.04.

Stabilizing mechanism: plant gain, controller gain and circulatory delay

There was no greater impact on $PACO_2-PICO_2$, plant gain or ventilation in cases of resolved versus persistent CSR (1% or 2% CO_2; P-value range: 0.3-0.8); thus, the stabilizing effects of inspired CO_2 occurred independently of CSR resolution.

Impact of sleep depth

Sleep efficiency (% sleep time; baseline: 62+4%) was not affected by 1% CO_2 (CO_2 versus baseline: −2±7%, P=0.4), 2% CO_2 (+4±4%, P=0.2) but was reduced with 3% CO_2 (−13±5%; P=0.02; RM ANOVA). Alpha EEG power (% total power; baseline: 18+2%) was not affected by 1% CO_2 (+1.6±1.4%, P=0.2), 2% CO_2 (−0.0±1.0%, P=0.4) or 3% CO_2 (+2.7±1.3%, P=0.054). Findings were similar when resolved and persistent CSR were assessed separately, i.e. resolved CSR did not accompany an improvement in sleep depth compared with persistent CSR. Neither baseline sleep efficiency nor baseline alpha power contributed significantly to predict the response to intervention when added to the logistic regression models described above (P=0.6 for both).

DISCUSSION

Alternative hypothesis: Proximity to the apnoeic threshold

A mean $PACO_2$ that is in close proximity to the apnoeic threshold (proximity theory) is commonly described as the mechanism responsible for CSR and its resolution with inspired CO_2. During CSR, large fluctuations in $PACO_2$ occur such that $PACO_2$ falls below the apnoeic threshold (ventilatory drive falls below zero; Figure S2a). Proximity theory suggests that raising mean $PACO_2$ would reduce an individual's susceptibility to a change in ventilation from causing CO_2 to pierce the apnoeic threshold and result in central apnoea (Figure S2b). However, this explanation for CSR inherently relies on an (unexplained) external source of fluctuations in ventilation or $PACO_2$ (e.g. via sleep-wake transitions) [S19], and thus cannot provide a stand-alone explanation for CSR. If fluctuations were driven by such an external source, then raising mean $PACO_2$ further away from the apnoeic threshold would prevent apnoea but $PACO_2$ oscillations would not be expected to resolve (Figure

S2b), yielding residual hypopneas. In contrast, we and others [S20, S21] invoke control theory (a reduction in loop gain) to explain CSR resolution, consistent with the observed suppression of oscillations in $PACO_2$ and ventilation (Figures 2, S3). Further analysis confirms that oscillations in $PACO_2$ and ventilation are indeed reduced substantially with inspired CO_2 when inspired CO_2 is expected to resolve CSR ($LG_{therapy}<0.8$) and when CSR is actually resolved; otherwise, oscillations remain (Figure S3). These findings are consistent with the control theory mechanism of CSR.

We also tested the quantitative predictive power of the proximity theory using a similar approach to that described for control theory. Specifically, we tested whether increased mean $PACO_2$ (by the group average of 1.7 mmHg per % inspired CO_2 during wake) and an accompanying increase in nadir $PACO_2$ of the same magnitude, would lead to resolved CSR when the expected nadir $PACO_2$ on therapy no longer reached the apnoeic threshold. The apnoeic threshold was calculated as the threshold value of $PACO_2$ that, based on the model $PACO_2$ signal, yielded an average apnoea duration matching that measured from the respiratory excursions signal (see example in Figure 2). The apnoeic threshold was measured from each 5 min baseline period prior to CO_2 intervention. We found that this model for CSR had a modest predictive power (Figure S4), largely as a consequence of a substantial proportion of occasions in which CSR resolved when the $PACO_2$ swings were expected to continue piercing the apnoeic threshold. This behaviour can be witnessed in the Figure 2 example trace: Note that if the cyclic 18 mmHg swings in $PACO_2$ (peak-to-trough) seen at baseline were also present on 2% CO_2 (Figure 1c), the apnoeic threshold—which lies ~5 mmHg below mean $PACO_2$—would have been traversed and CSR would have persisted; by contrast, CSR was resolved.

Alternative hypothesis: Central pattern generator

Here we address the possibility that Cheyne-Stokes respiration is caused by central/neural pacemaker mechanisms (i.e. an intrinsic rhythm [S22-24]), independent from ventilatory chemoreflex mechanisms involving feedback. If true, then:

1.) the cycle duration of Cheyne-Stokes respiration would be determined by the timing properties of respiratory control centre interactions, whereas the cycle duration is strongly dependent on the circulation time between the lungs and the chemoreceptors [S4, S25-27].

2.) the application of dynamic inspired CO_2 to clamp $PACO_2$ can diminish or abolish CSR, but would not be expected to do so if CSR were driven by a source independent of feedback [S28]. It is clear that the (ventilatory feedback-induced) fluctuations in $PACO_2$ are needed for the ventilatory fluctuations of CSR.

One might also postulate that inspired CO_2, via increased $PACO_2$, could saturate chemoreceptor circuits such that ventilation becomes large and insensitive to dips in CO_2. This should be observed in the form of a reduced chemosensitivity or controller gain (ratio of the magnitude of swings in ventilatory drive to those in $PACO_2$). By contrast, our finding that inspired CO_2 ($\leq$3%) does not alter the chemosensitivity indicates otherwise. We note that the increase in ventilation with 3% inspired CO_2 (+57±25%$_{mean}$, mean±S.D.) was small relative to the size of the peak ventilation that occurred during baseline CSR (230±68%$_{mean}$). Thus the operating point was not shifted beyond the range in which ventilation can be seen to vary sensitively with swings in $PACO_2$. Hence, our data do not provide evidence to suggest the saturation and accompanying desensitization of chemoreceptor inputs with inspired CO_2.

Methodological considerations: Non-linearities

Previous investigators have cautioned that the value of loop gain may change as the size of the ventilatory oscillation grows and CSR is established [S3, S6]. Indeed we know that at eupnea an unstable system with a eupneic loop gain of 1.4 will have an *overall loop gain* of 1 during CSR, based on the observation that oscillations neither grow nor decay [S5, S6]. However, our measure of baseline loop gain seeks to reveal the underlying linear loop gain (e.g. 1.4) by taking into account the non-linear impact of piercing the apneic threshold [S5]. However, it remains possible that this underlying linear loop gain observed during CSR, which reflects the magnitude of ventilatory drive response to a large perturbation in ventilation, differs considerably

from the loop gain near eupnea, e.g. due to apnea-related hypoxia. We feel this is unlikely for the following reasons:

- Our previous modelling study illustrated that the loop gain during CSR (the underlying linear component) was virtually identical to the loop gain near eupnea [S5].
- Our finding that controller gain was unchanged with effective CO_2 intervention (which reduces the range of ventilation values about which the controller gain was measured) suggests this any increase/decrease in controller gain is likely to be relatively small.
- Substantial non-linear effects, if present, should be evident in the form of a substantial departure from the characteristic crescendo-decrescendo ventilatory pattern of CSR (sinusoidal ventilatory oscillation truncated by apnea).

We note that other methods to assess ventilatory control, including pseudo-random binary stimulation [S16, S29], hypercapnic ventilatory responses measured above or below eupnea [S9, S30], proportional assist ventilation [S31, S32], CPAP manipulation [S33-36], and model-fitting to spontaneous OSA data [S15], have similarly assumed approximate linearity across a sizable range of ventilation and CO_2 values and have provided physiological insight.

Perhaps most importantly, baseline loop gain is measured across the range of ventilation and CO_2 levels that may matter most for predicting responses to therapy. If the underlying loop gain is somewhat larger during the ventilatory swings of CSR (compared with loop gain near eupnea) it would be this larger value that needs to be moved below 1 to acutely resolve CSR and to protect against its re-emergence with large perturbations.

Methodological considerations: End-tidal PCO_2 as an estimate of alveolar and arterial PCO_2.

End-tidal PCO_2 is an established means to estimate the alveolar PCO_2 ($PACO_2$) at it represents the ventilation-weighted average of the alveolar gas [S37-39]. End-tidal PCO_2 is used ubiquitously in studies of ventilatory control in patients with and without heart failure to reflect changes to arterial PCO_2 on a breath-to-breath time

scale [S7, S28, S30, S40-42]. Available alternatives, including arterial blood gas sampling and transcutaneous PCO_2, are unsuitable for assessing arterial PCO_2 dynamics due to insufficient time resolution and marked damping of PCO_2 transients by the tissues/skin surface respectively [S7].

In principle, it is the difference in inspired and alveolar PCO_2 (rather than arterial PCO_2) that determines the CO_2 excretion at the mouth and thus the plant gain (Equation S1). As such, through the measurement of end-tidal PCO_2 we are estimating the primary variable of interest (alveolar PCO_2). For the measurements of plant and controller gain, however, we assume that swings in $PACO_2$ reflect proportional swings in arterial PCO_2 which in turn are responsible for the ventilatory chemoreflex feedback responses, as commonly assumed [S28, S30, S40-42]. Although the difference between $PACO_2$ and arterial PCO_2 may be considerable in some patients with heart failure (e.g. via ventilation-perfusion heterogeneity associated with pulmonary congestion), we note that a constant discrepancy between these two variables will have no impact on the absolute values of plant and controller gain reported as both are measures that reflect PCO_2 changes (Table 1). Moreover, the changes in plant and controller gain with intervention are also presented as percentage changes from baseline; thus a proportional discrepancy (i.e. $PACO_2 = m \times$ arterial $PCO_2 + c$) will also have no impact on the results presented (Figure 4) or our conclusions. It is reasonable to assume negligible changes in pulmonary function with intervention.

The values of end-tidal PCO_2 measured in the current study (30.6±2.6 mmHg), are approximately 25% lower than in patients without heart failure or CSR (40 mmHg [S35]), which may raise doubts as to the reliability of the $PACO_2$ values obtained. We note, however, that patients with heart failure and severe central sleep apnea are a population known to exhibit severe hypocapnia (arterial PCO_2 as low as 33 mmHg in previous studies [S26]). End-tidal PCO_2 values are also typically 1-5 mmHg lower than arterial values in healthy adults [S39], and the difference may be even greater in patients with heart failure and subclinical pulmonary congestion [S43-45]. Note that in the example traces provided by Lorenzi-Filho et al [S7] during CSR, mean end-tidal/alveolar

PCO_2 levels range from ~25-30 mmHg whereas transcutaneous PCO_2 range from 30-35 mmHg. Thus, overall, the end-tidal PCO_2 values we report are consistent with the literature.

We also note that patients with heart failure and severe central sleep apnea often exhibit a substantial degree of hyperventilation as the cause of their hypocapnia. For example, Naughton et al's arterial PCO_2 values of 33 mmHg coincided with a high minute ventilation of 8.3 L/min [S26]. In the current study, patients exhibited a profound elevation in minute ventilation, on average 11.2 L/min of ventilation, representing a 60% increase over a typical ventilation of 7 L/min [S35]. Thus the magnitude of observed hypocapnia is consistent with the degree of hyperventilation.

Also consistent with the low end-tidal PCO_2 values observed, we also found an elevated end-tidal PO_2 in our study group (113.2±5.3 mmHg), which represents an increase from normal (100 mmHg) by an amount (13.2 mmHg) that is concordant with the observed reduction in PCO_2 (9.4 mmHg). That is, if we assume a respiratory exchange ratio of 0.8, the end-tidal PCO_2 value that we would predict using end-tidal PO_2 alone would be $(150-113.2)\times 0.8 = 29.4$ mmHg, consistent with the values reported.

A further important test of the validity of our use of end-tidal $PETCO_2$ to reflect changes in $PACO_2$ is whether the values of $PACO_2$ were correlated as expected with the observed changes in ventilation. Dynamic swings in ventilation will cause a transient opposing fluctuation in alveolar $PACO_2$ that is slightly damped by the lung gas stores. Fitting a differential equation to describe this physiology (Equation S3) revealed that inter-breath fluctuations in ventilation correlated remarkably with those in end-tidal CO_2 (R=0.94 on average). The inter-breath accuracy of this simple model fit can be seen in Figure 2. The observation that the changes in end-tidal PCO_2 captured the expected changes in $PACO_2$ driven by ventilation confirms the appropriateness of end-tidal PCO_2 as a measure of $PACO_2$.

Methodological considerations: Controller gain values

Our data illustrate that controller gain was unchanged with inspired CO_2 intervention. No attempt was made to ascertain whether the controller gain measurements were driven primarily by central chemoreflexes or

carotid/peripheral chemoreflexes (their complex interaction is considered to render separate assessment unfeasible [S46]) or to ascertain whether there was any (additive or interactive) involvement of the attendant swings in PO_2. We also did not attempt to subtract out the influence of sleep-wake transitions, which may act to augment the measured controller gain [S47-53]. Thus the controller gain measurement reflects the combined influence of multiple potential mechanisms that act in concert with the change in $PACO_2$ to elicit a reflex ventilatory response. Nonetheless, as we found no change in this measure with CO_2 intervention, it is unlikely that any important component of the overall ventilatory response to CO_2 was altered.

The values for controller gain observed during CSR we measured (~2 L/min/mmHg) are not as large as some of those estimated using rebreathing or steady-state methods [S9, S30, S40], although they are comparable with values obtained by others [S42]. The explanation lies with the concept that short-term (i.e. dynamic) ventilatory responses to CO_2 yield chemoreflex values that are far smaller than longer-term steady-state methods [S40]. In principle, dynamic fluctuations in $PACO_2$—including those taken *in situ* during CSR in the current study—do not allow time for the ventilatory response to develop fully before the stimulus is withdrawn and reversed, therefore yielding lower values.

Predictive utility compared to the apnoea-hypopnoea index

In patients with heart failure, the apnoea-hypopnoea index (AHI) has been observed to be slightly greater in responders to CPAP therapy versus non-responders [S54]. However, this relationship is weak [S5], and thus baseline AHI is accepted as having little value for the prediction of responses to therapy in patients with heart failure and CSR. Likewise in the current study, we find a non-significant association between loop gain and AHI during NREM sleep (R=0.49, P=0.11). This modest relationship is, in fact, largely expected: Once patients exhibit CSR most of the time, the magnitude of loop gain will weakly determine the frequency of events (instead the cycle period will explain the AHI). For example a patient with continuous CSR and a cycle length of 2 min will have an AHI of 60/2 = 30 events/hr (even if loop gain is 1.1). Another patient with a loop gain of 1.8 may have a cycle length of 0.75 min and will therefore have an AHI of 60/0.75=80 events/hr. At least

amongst patients with persistent CSR for a large proportion of the night, the link between AHI and LG is modest.

On the other hand, in our study group we noticed a significant relationship between loop gain (research polysomnography, baseline prior to CO_2 intervention) and the central apnoea index (clinical polysomnography) in our study group (R=0.76, P=0.004) as well as an association between loop gain and the percentage of central events (R=0.65, P=0.02). It is possible that these two parameters, as manifestations of higher loop gain amongst patients with severe CSR, may have some predictive value to guide therapeutic interventions. Prospectively evaluating the relationship between loop gain and polysomnographic features of CSR in a larger sample is likely to be of clinical interest.

Further clinical implications

The use of respiratory stimulants to raise ventilation and lower $PACO_2-PICO_2$, and thereby to improve CSR, remains of major interest to clinical investigators [S7, S8, S55, S56]. Inspired CO_2, for example, can ameliorate CSR in all patients, suggesting an important advantage in effectiveness over other therapies (e.g. CPAP, supplemental oxygen) that are typically effective in those with a milder ventilatory control instability [S5]. Respiratory stimulation in the form of added dead space can also resolve CSR in most patients with heart failure [S57]; of note the 0.25 L of dead space that was used in the study by Khayat *et al.* raises inspired CO_2 by ~2%, a level that was often effective at resolving CSR in the current study. Pharmacological stimulants including acetazolamide and theophylline can resolve CSR in some patients with heart failure [S55, S56, S58, S59], just as they can improve CSR in healthy adults at high altitude and in infants in neonatal intensive care [S59-61]. In heart failure, respiratory stimulants for CSR can reduce the frequency of ectopic beats [S8], improve perception of sleep quality [S56], and may be preferred over positive pressure therapies in some individuals [S62].

TABLES

TABLE S1. LOGISTIC REGRESSION: BASELINE LOOP GAIN ADJUSTING FOR INSPIRED CO_2

Variable	Coefficient	Standard Error	Wald Statistic	P value	VIF	Odds Ratio (95%C.I.)
Baseline loop gain	-7.802	2.339	11.129	<0.001	1.003	4.1×10^{-4} (4.2×10^{-6}–0.04)
Inspired CO_2 ($FICO_2$)	3.942	0.871	20.498	<0.001	1.003	51 (9–284)

Likelihood Ratio Test Statistic: 71.024 (P = <0.001).
Model accuracy = 88%.
Regression equation: P = 3.9−7.8×[Baseline loop gain]+3.9×$FICO_2$

TABLE S2. LOGISTIC REGRESSION: BASELINE LOOP GAIN ADJUSTING FOR INSPIRED CO_2 AND SUBJECTS

Variable	Coefficient	Standard Error	Wald Statistic	P value	VIF	Odds Ratio (95%C.I.)
Baseline loop gain	-14.726	4.988	8.715	0.003	2.411	4.0×10^{-7} (2.3×10^{-11}–0.007)
Inspired CO_2 ($FICO_2$)	5.748	1.635	12.363	<0.001	1.511	314 (13–7727)

Likelihood Ratio Test Statistic: 90.095 (P = <0.001).
Model accuracy = 83%.
Regression equation: P = 22.9−14.7×[Baseline loop gain]+5.7×$FICO_2$−12.0×Subject2−14.7×Subject3−10.4×Subject4 −13.9×Subject5−15.2×Subject6−15.3×Subject7−10.0×Subject8−6.3×Subject9−8.1×Subject10−3.1×Subject11 −14.2×Subject12
Subject effects are referenced to Subject1. All P values for Subject were >0.95.

FIGURES

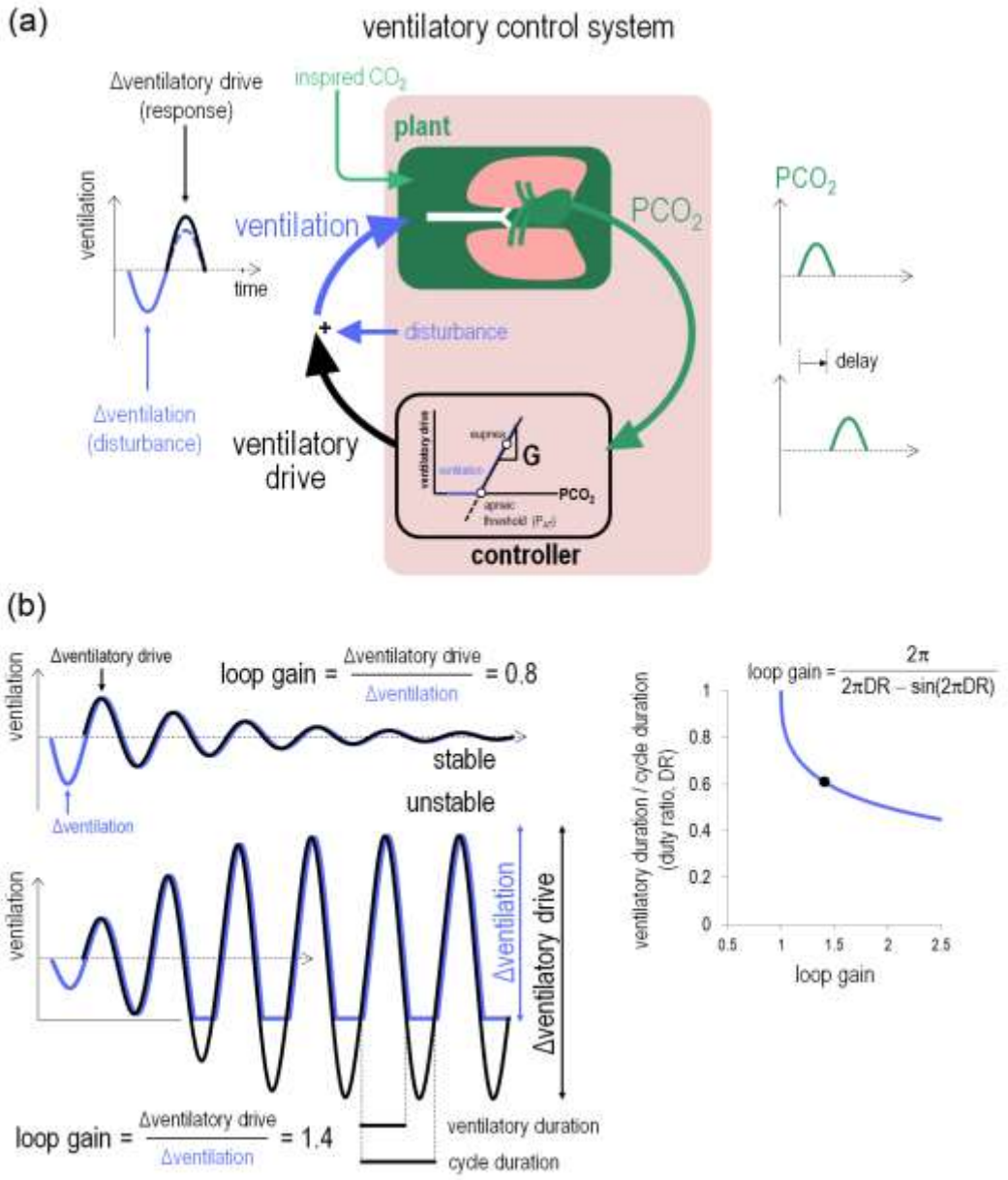

Figure S1. Control theory explanation for Cheyne-Stokes respiration (CSR). (**a**) Schematic of the negative feedback loop controlling ventilation. Loop gain is the ventilatory drive response to a change in ventilation. Note that loop gain is the product of the plant gain and the controller gain; both are possible causes of instability and potential avenues for intervention (see Equation S1). (**b**) Loop gain <1 leads to decaying oscillations such that ventilation is stable. Loop gain >1 leads to oscillatory growth until CSA is established; the system is unstable*. In this example, when loop gain is 1.4, the swings in ventilatory drive (black) are 40% larger than the swings in ventilation (blue). Loop gain therefore determines the magnitude and duration of the reduction in ventilatory drive below the apneic threshold, and can be calculated from the ratio of ventilatory duration to cycle duration based on trigonometry (inset). Theoretically, the pattern of CSR reflects the degree of instability and thus should predict the therapeutic reduction in loop gain needed for CSR resolution. *The instability criterion (LG>1) applies strictly at the characteristic cycle duration of the feedback loop, e.g. the cycle duration of CSR. For disturbances at this characteristic cycle duration, the ventilatory response is time-shifted by half a cycle such that it becomes *in phase* with the disturbance (panel **a**). Figure summarises previous work [S1-3, S5].

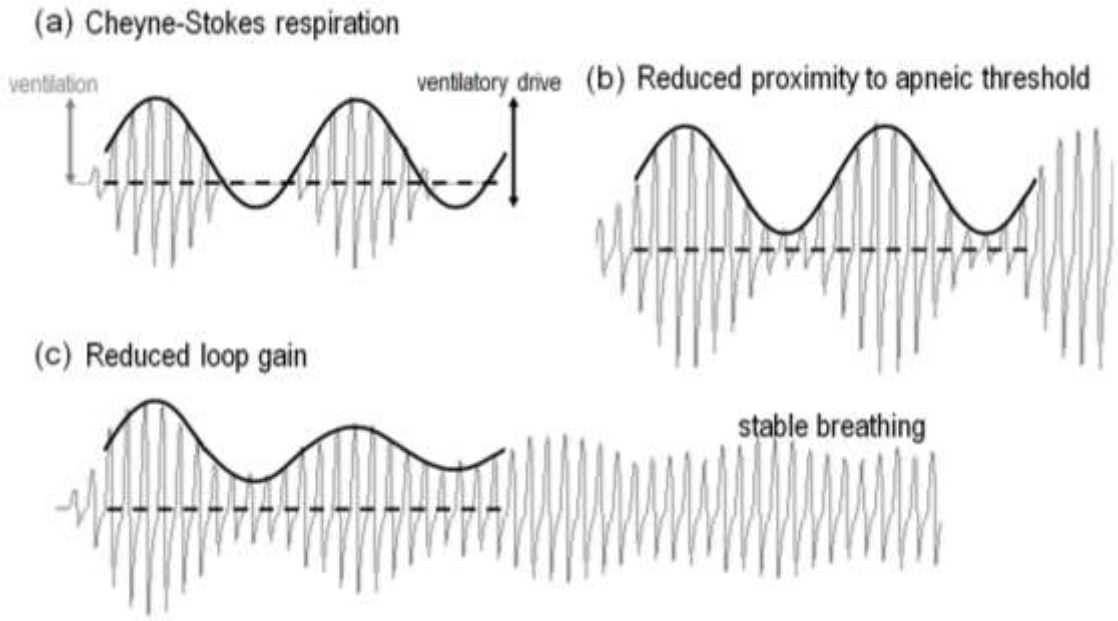

Figure S2. Competing hypotheses: the mechanism of Cheyne-Stokes respiration. (**a**) Illustration of ventilation and ventilatory drive swings during Cheyne-Stokes respiration (CSR), showing sub-threshold ventilatory drive (as arterial PCO_2 falls below the apnoeic threshold) to yield central apnoeas. Two mechanisms have been invoked to explain the occurrence of CSR and its resolution with inspired CO_2 stimulation: (**b**) Increasing eupneic arterial PCO_2 away from the apnoeic threshold may prevent a given PCO_2 and ventilatory drive oscillation from yielding apnoea, but would not explain a reduced magnitude of ventilatory oscillation. (**c**) Control theory states that a sufficient reduction of loop gain (e.g. consequent to a reduced alveolar-inspired PCO_2 gradient for CO_2 elimination; Equation S1) removes the source of ventilatory oscillations and resolves CSR.

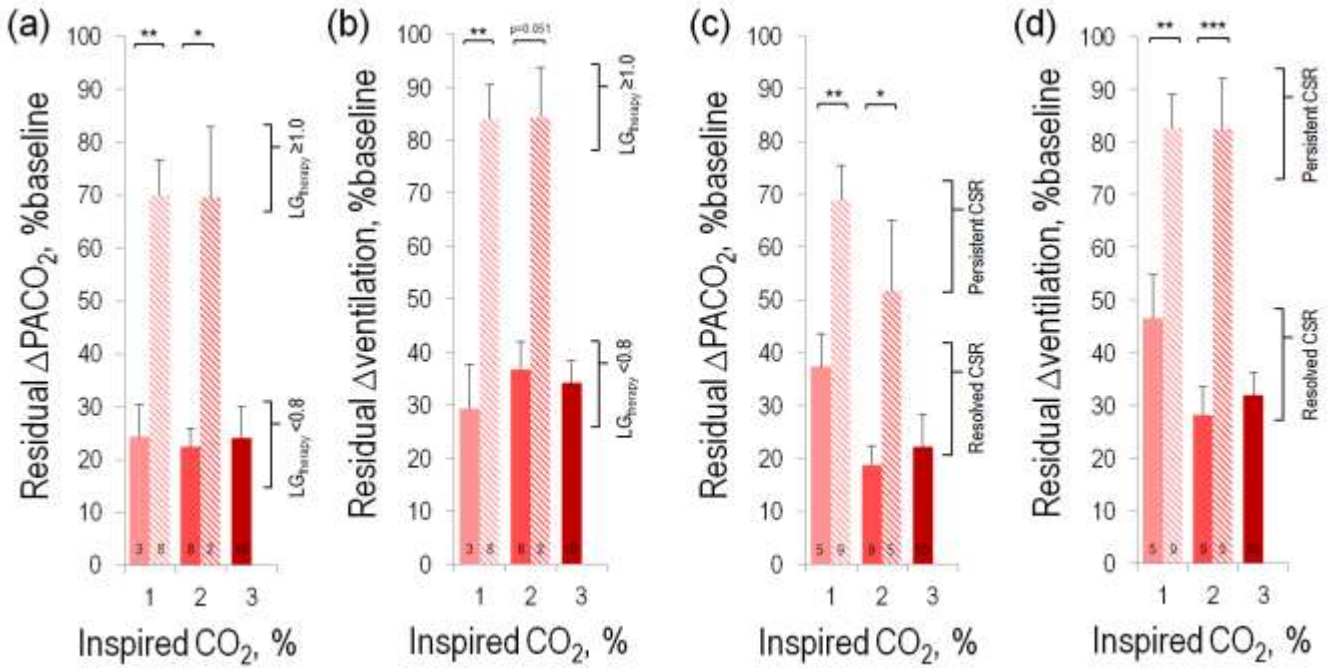

Figure S3. Reduced magnitude of $PACO_2$ and ventilatory oscillations with effective CSR intervention. Swings in $PACO_2$ (**a**) and ventilation (**b**) are reduced substantially with inspired CO_2 when loop gain can be lowered below 0.8 ($LG_{therapy}<0.8$) but minimally when loop gain remains above 1.0 ($LG_{therapy}\geq1.0$). A similar effect is observed comparing resolved versus persistent CSR (**c** and **d**). Solid bars indicate changes accompanying CSR resolution (predicted in panels a-b, actual in panels c-d) whereas hatched bars indicate changes accompanying CSR persistence. Data were taken 5 min after commencing inspired CO_2 and presented as percent of baseline. Fluctuations were quantified by fitting a sinusoid using Fourier integration. *p<0.05, **p<0.01, ***p<0.001 Student's t-tests, unpaired. The number of patients contributing data for each comparison is shown in each bar. Baseline $PACO_2$ and ventilatory oscillations had a mean amplitude (peak-to-trough) of 10.0±2.1 mmHg and 23.9±7.8 L/min respectively (mean±S.E.M.).

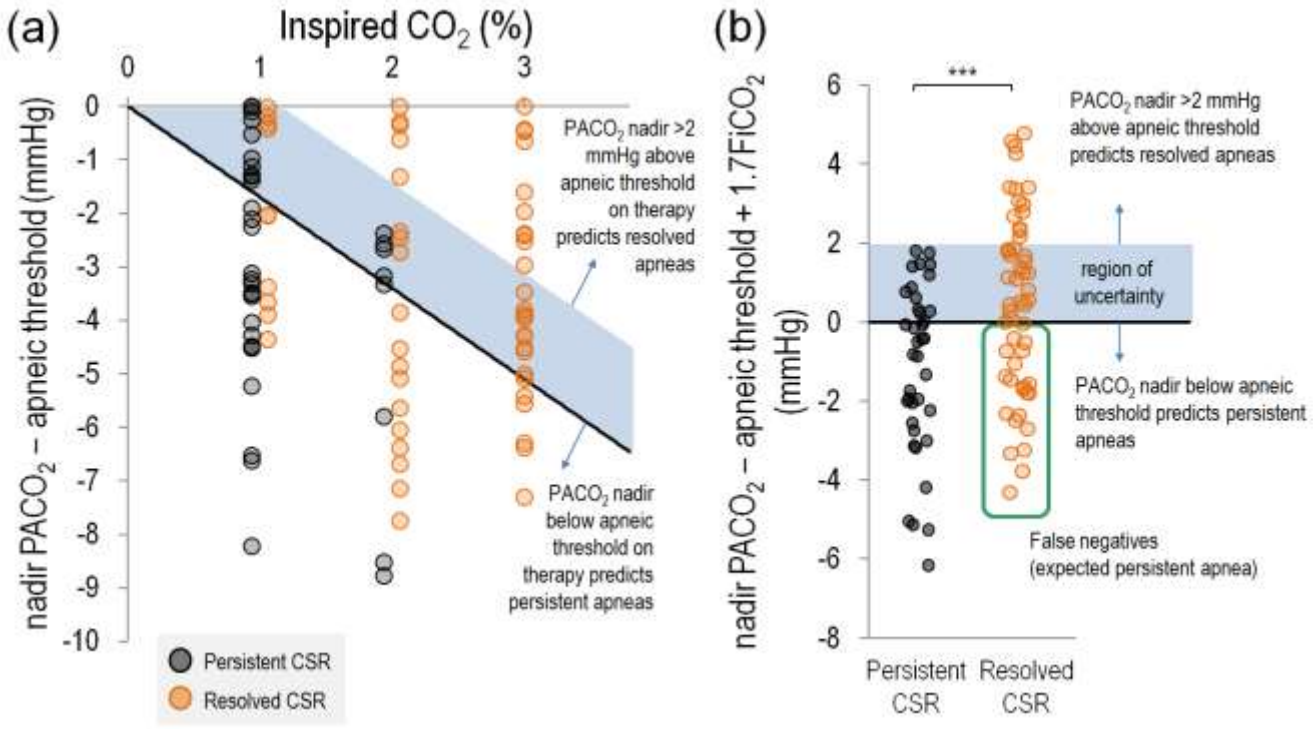

Figure S4. Raising mean $PACO_2$ away from the PCO_2 apnoeic threshold (proximity theory) has a limited capacity to predict the resolution of Cheyne-Stokes respiration (CSR) with inspired CO_2 stimulation. Here we test the theory that CSR will resolve if the expected rise in mean $PACO_2$ (1.7 mmHg per % inspired CO_2) would prevent the swing in $PACO_2$ from piercing the PCO_2 apnoeic threshold. That is, a nadir $PACO_2$ that is far below the apnoeic threshold would require a greater increase in mean $PACO_2$ to prevent apnoea. (**a**) The nadir $PACO_2$ was not significantly further below the apnoeic threshold prior to epochs of persistent CSR than epochs of resolved CSR ($P>0.15$). The solid line reflects a predicted nadir $PACO_2$ = apnoeic threshold on therapy. (**b**) Combining data for 1, 2, and 3% CO_2 shows that the predicted nadir $PACO_2$ – apnoeic threshold on therapy is higher in resolved CSR persistent vs. resolved CSR. There was, however, a considerable proportion (41%) of resolved CSR that occurred despite predicted CSR persistence (false negatives in green rectangle).

REFERENCES

S1. Sands SA, Owens RL. Congestive heart failure and central sleep apnea. *Critical care clinics* 2015: 31(3): 473-495.

S2. Edwards BA, Sands SA, Berger PJ. Postnatal maturation of breathing stability and loop gain: the role of carotid chemoreceptor development. *Respir Physiol Neurobiol* 2013: 185(1): 144-155.

S3. Khoo MC, Kronauer RE, Strohl KP, Slutsky AS. Factors inducing periodic breathing in humans: a general model. *J Appl Physiol* 1982: 53(3): 644-659.

S4. Francis DP, Willson K, Davies LC, Coats AJ, Piepoli M. Quantitative general theory for periodic breathing in chronic heart failure and its clinical implications. *Circulation* 2000: 102(18): 2214-2221.

S5. Sands SA, Edwards BA, Kee K, Turton A, Skuza EM, Roebuck T, O'Driscoll DM, Hamilton GS, Naughton MT, Berger PJ. Loop gain as a means to predict a positive airway pressure suppression of Cheyne-Stokes respiration in patients with heart failure. *Am J Respir Crit Care Med* 2011: 184(9): 1067-1075.

S6. Khoo MCK. Nonlinear analysis of physiological control systems. *In:* Herrick RJ, ed. Physiological control systems Analysis, simulation, and estimation. John Wiley & Sons, Inc., New Jersey, 2000; pp. 229-269.

S7. Lorenzi-Filho G, Rankin F, Bies I, Douglas Bradley T. Effects of inhaled carbon dioxide and oxygen on cheyne-stokes respiration in patients with heart failure. *Am J Respir Crit Care Med* 1999: 159(5 Pt 1): 1490-1498.

S8. Leung RS, Diep TM, Bowman ME, Lorenzi-Filho G, Bradley TD. Provocation of ventricular ectopy by cheyne-stokes respiration in patients with heart failure. *Sleep* 2004: 27(7): 1337-1343.

S9. Xie A, Skatrud JB, Puleo DS, Rahko PS, Dempsey JA. Apnea-hypopnea threshold for CO2 in patients with congestive heart failure. *Am J Respir Crit Care Med* 2002: 165(9): 1245-1250.

S10. Szollosi I, Jones M, Morrell MJ, Helfet K, Coats AJ, Simonds AK. Effect of CO2 inhalation on central sleep apnea and arousals from sleep. *Respiration* 2004: 71(5): 493-498.

S11. Steens RD, Millar TW, Su X, Biberdorf D, Buckle P, Ahmed M, Kryger MH. Effect of inhaled 3% CO2 on Cheyne-Stokes respiration in congestive heart failure. *Sleep* 1994: 17(1): 61-68.

S12. Andreas S, Weidel K, Hagenah G, Heindl S. Treatment of Cheyne-Stokes respiration with nasal oxygen and carbon dioxide. *Eur Respir J* 1998: 12(2): 414-419.

S13. Nemati S, Edwards BA, Sands SA, Berger PJ, Wellman A, Verghese GC, Malhotra A, Butler JP. Model-based characterization of ventilatory stability using spontaneous breathing. *J Appl Physiol* 2011: 111(1): 55-67.

S14. Gederi E, Nemati S, Edwards BA, Clifford GD, Malhotra A, Wellman A. Model-based estimation of loop gain using spontaneous breathing: a validation study. *Respir Physiol Neurobiol* 2014: 201: 84-92.

S15. Terrill PI, Edwards BA, Nemati S, Butler JP, Owens RL, Eckert DJ, White DP, Malhotra A, Wellman A, Sands SA. Quantifying the ventilatory control contribution to sleep apnoea using polysomnography. *Eur Respir J* 2015: 45(2): 408-418.

S16. Ghazanshahi SD, Khoo MC. Estimation of chemoreflex loop gain using pseudorandom binary CO2 stimulation. *IEEE Trans Biomed Eng* 1997: 44(5): 357-366.

S17. Khoo MC, Yang F, Shin JJ, Westbrook PR. Estimation of dynamic chemoresponsiveness in wakefulness and non-rapid-eye-movement sleep. *J Appl Physiol* 1995: 78(3): 1052-1064.

S18. Gleeson K, Zwillich CW, White DP. The influence of increasing ventilatory effort on arousal from sleep. *Am Rev Respir Dis* 1990: 142(2): 295-300.

S19. Javaheri S. Central sleep apnea. *Clin Chest Med* 2010: 31(2): 235-248.

S20. Rapoport DM. Stabilizing ventilation in OSAHS with CPAP emergent periodic breathing through the use of dead space. *J Clin Sleep Med* 2010: 6(6): 539-540.

S21. Manisty CH, Willson K, Wensel R, Whinnett ZI, Davies JE, Oldfield WL, Mayet J, Francis DP. Development of respiratory control instability in heart failure: a novel approach to dissect the pathophysiological mechanisms. *J Physiol* 2006: 577(Pt 1): 387-401.

S22. Franklin KA, Sandstrom E, Johansson G, Balfors EM. Hemodynamics, cerebral circulation, and oxygen saturation in Cheyne-Stokes respiration. *J Appl Physiol* 1997: 83(4): 1184-1191.

S23. Hoff HE, Breckenridge CG. Intrinsic mechanisms in periodic breathing. *AMA archives of neurology and psychiatry* 1954: 72(1): 11-42.

S24. Umantsev A, Golbin A. Correlations of physiological activities in nocturnal Cheyne-Stokes respiration. *Nature and science of sleep* 2011: 3: 21-32.

S25. Hall MJ, Xie A, Rutherford R, Ando S, Floras JS, Bradley TD. Cycle length of periodic breathing in patients with and without heart failure. *Am J Respir Crit Care Med* 1996: 154(2 Pt 1): 376-381.

S26. Naughton M, Benard D, Tam A, Rutherford R, Bradley TD. Role of hyperventilation in the pathogenesis of central sleep apneas in patients with congestive heart failure. *Am Rev Respir Dis* 1993: 148(2): 330-338.

S27. Murphy RM, Shah RV, Malhotra R, Pappagianopoulos PP, Hough SS, Systrom DM, Semigran MJ, Lewis GD. Exercise oscillatory ventilation in systolic heart failure: an indicator of impaired hemodynamic response to exercise. *Circulation* 2011: 124(13): 1442-1451.

S28. Giannoni A, Baruah R, Willson K, Mebrate Y, Mayet J, Emdin M, Hughes AD, Manisty CH, Francis DP. Real-time dynamic carbon dioxide administration: a novel treatment strategy for stabilization of periodic breathing with potential application to central sleep apnea. *J Am Coll Cardiol* 2010: 56(22): 1832-1837.

S29. Hudgel DW, Gordon EA, Thanakitcharu S, Bruce EN. Instability of ventilatory control in patients with obstructive sleep apnea. *Am J Respir Crit Care Med* 1998: 158(4): 1142-1149.

S30. Javaheri S. A mechanism of central sleep apnea in patients with heart failure. *N Engl J Med* 1999: 341(13): 949-954.

S31. Meza S, Giannouli E, Younes M. Control of breathing during sleep assessed by proportional assist ventilation. *J Appl Physiol* 1998: 84(1): 3-12.

S32. Wellman A, Malhotra A, Fogel RB, Edwards JK, Schory K, White DP. Respiratory system loop gain in normal men and women measured with proportional-assist ventilation. *J Appl Physiol* 2003: 94(1): 205-212.

S33. Wellman A, Eckert DJ, Jordan AS, Edwards BA, Passaglia CL, Jackson AC, Gautam S, Owens RL, Malhotra A, White DP. A method for measuring and modeling the physiological traits causing obstructive sleep apnea. *J Appl Physiol* 2011: 110(6): 1627-1637.

S34. Wellman A, Edwards BA, Sands SA, Owens RL, Nemati S, Butler J, Passaglia CL, Jackson AC, Malhotra A, White DP. A simplified method for determining phenotypic traits in patients with obstructive sleep apnea. *J Appl Physiol* 2013: 114(7): 911-922.

S35. Edwards BA, Sands SA, Eckert DJ, White DP, Butler JP, Owens RL, Malhotra A, Wellman A. Acetazolamide improves loop gain but not the other physiological traits causing obstructive sleep apnoea. *J Physiol* 2012: 590(Pt 5): 1199-1211.

S36. Eckert DJ, White DP, Jordan AS, Malhotra A, Wellman A. Defining phenotypic causes of obstructive sleep apnea. Identification of novel therapeutic targets. *Am J Respir Crit Care Med* 2013: 188(8): 996-1004.

S37. Tobin MJ. Respiratory monitoring in the intensive care unit. *Am Rev Respir Dis* 1988: 138(6): 1625-1642.

S38. Benumof JL. Interpretation of capnography. *AANA journal* 1998: 66(2): 169-176.

S39. Rahn H. A concept of mean alveolar air and the ventilation-blood flow relationships during pulmonary gas exchange. *Am J Physiol* 1949: 158(1): 21-30.

S40. Solin P, Roebuck T, Johns DP, Walters EH, Naughton MT. Peripheral and central ventilatory responses in central sleep apnea with and without congestive heart failure. *Am J Respir Crit Care Med* 2000: 162(6): 2194-2200.

S41. Topor ZL, Johannson L, Kasprzyk J, Remmers JE. Dynamic ventilatory response to CO(2) in congestive heart failure patients with and without central sleep apnea. *J Appl Physiol* 2001: 91(1): 408-416.

S42. Giannoni A, Emdin M, Bramanti F, Iudice G, Francis DP, Barsotti A, Piepoli M, Passino C. Combined increased chemosensitivity to hypoxia and hypercapnia as a prognosticator in heart failure. *J Am Coll Cardiol* 2009: 53(21): 1975-1980.

S43. Szollosi I, Thompson BR, Krum H, Kaye DM, Naughton MT. Impaired pulmonary diffusing capacity and hypoxia in heart failure correlates with central sleep apnea severity. *Chest* 2008: 134(1): 67-72.

S44. Kee K, Stuart-Andrews C, Ellis MJ, Wrobel JP, Nilsen K, Sharma M, Thompson BR, Naughton MT. Increased Dead Space Ventilation Mediates Reduced Exercise Capacity in Systolic Heart Failure. *Am J Respir Crit Care Med* 2016.

S45. Kee K, Stuart-Andrews C, Nilsen K, Wrobel JP, Thompson BR, Naughton MT. Ventilation heterogeneity is increased in patients with chronic heart failure. *Physiological reports* 2015: 3(10).

S46. Smith CA, Blain GM, Henderson KS, Dempsey JA. Peripheral chemoreceptors determine the respiratory sensitivity of central chemoreceptors to CO2 : role of carotid body CO2. *J Physiol* 2015: 593(18): 4225-4243.

S47. Dunai J, Wilkinson M, Trinder J. Interaction of chemical and state effects on ventilation during sleep onset. *J Appl Physiol* 1996: 81(5): 2235-2243.

S48. Trinder J, Merson R, Rosenberg JI, Fitzgerald F, Kleiman J, Douglas Bradley T. Pathophysiological interactions of ventilation, arousals, and blood pressure oscillations during cheyne-stokes respiration in patients with heart failure. *Am J Respir Crit Care Med* 2000: 162(3 Pt 1): 808-813.

S49. Douglas NJ, White DP, Weil JV, Pickett CK, Zwillich CW. Hypercapnic ventilatory response in sleeping adults. *Am Rev Respir Dis* 1982: 126(5): 758-762.

S50. Trinder J, Ivens C, Kleiman J, Kleverlaan D, White DP. The cardiorespiratory activation response at an arousal from sleep is independent of the level of CO(2). *J Sleep Res* 2006: 15(2): 174-182.

S51. Skatrud JB, Dempsey JA. Interaction of sleep state and chemical stimuli in sustaining rhythmic ventilation. *Journal of applied physiology: respiratory, environmental and exercise physiology* 1983: 55(3): 813-822.

S52. Pinna GD, Maestri R, Mortara A, La Rovere MT. Cardiorespiratory interactions during periodic breathing in awake chronic heart failure patients. *Am J Physiol Heart Circ Physiol* 2000: 278(3): H932-941.

S53. Mahamed S, Ali AF, Ho D, Wang B, Duffin J. The contribution of chemoreflex drives to resting breathing in man. *Exp Physiol* 2001: 86(1): 109-116.

S54. Arzt M, Floras JS, Logan AG, Kimoff RJ, Series F, Morrison D, Ferguson K, Belenkie I, Pfeifer M, Fleetham J, Hanly P, Smilovitch M, Ryan C, Tomlinson G, Bradley TD. Suppression of central sleep apnea by continuous positive airway pressure and transplant-free survival in heart failure: a post hoc analysis of the Canadian Continuous Positive Airway Pressure for Patients with Central Sleep Apnea and Heart Failure Trial (CANPAP). *Circulation* 2007: 115(25): 3173-3180.

S55. Javaheri S, Parker TJ, Wexler L, Liming JD, Lindower P, Roselle GA. Effect of theophylline on sleep-disordered breathing in heart failure. *N Engl J Med* 1996: 335(8): 562-567.

S56. Javaheri S. Acetazolamide improves central sleep apnea in heart failure: a double-blind, prospective study. *Am J Respir Crit Care Med* 2006: 173(2): 234-237.

S57. Khayat RN, Xie A, Patel AK, Kaminski A, Skatrud JB. Cardiorespiratory effects of added dead space in patients with heart failure and central sleep apnea. *Chest* 2003: 123(5): 1551-1560.

S58. Hu K, Li Q, Yang J, Hu S, Chen X. The effect of theophylline on sleep-disordered breathing in patients with stable chronic congestive heart failure. *Chinese medical journal* 2003: 116(11): 1711-1716.

S59. Fischer R, Lang SM, Leitl M, Thiere M, Steiner U, Huber RM. Theophylline and acetazolamide reduce sleep-disordered breathing at high altitude. *Eur Respir J* 2004: 23(1): 47-52.

S60. Davi MJ, Sankaran K, Simons KJ, Simons FE, Seshia MM, Rigatto H. Physiologic changes induced by theophylline in the treatment of apnea in preterm infants. *J Pediatr* 1978: 92(1): 91-95.

S61. Finer NN, Peters KL, Duffley LM, Coward JH. An evaluation of theophylline for idiopathic apnea of infancy. *Developmental pharmacology and therapeutics* 1984: 7(2): 73-81.

S62. Thomas RJ. Effect of added dead space to positive airway pressure for treatment of complex sleep-disordered breathing. *Sleep Med* 2005: 6(2): 177-178.